NACA RM A50F13

NACA

RESEARCH MEMORANDUM

AN EXPERIMENTAL INVESTIGATION AT LARGE SCALE OF AN NACA SUBMERGED INTAKE AND DEFLECTOR INSTALLATION ON THE REARWARD PORTION OF A FUSELAGE

By Curt A. Holzhauser

Ames Aeronautical Laboratory
Moffett Field, Calif.

NATIONAL ADVISORY COMMITTEE
FOR AERONAUTICS

WASHINGTON

August 30, 1950
Declassified June 20, 1957

NATIONAL ADVISORY COMMITTEE FOR AERONAUTICS

RESEARCH MEMORANDUM

AN EXPERIMENTAL INVESTIGATION AT LARGE SCALE OF AN NACA SUBMERGED INTAKE AND DEFLECTOR INSTALLATION ON THE REARWARD PORTION OF A FUSELAGE

By Curt A. Holzhauser

SUMMARY

The results of an experimental investigation at low speed to determine the pressure-recovery and drag characteristics of an NACA submerged intake and deflector installation on the rearward portion of the fuselage of a model are presented.

The entrance ram-recovery ratio of the intake in this investigation was between 0 and 0.05 lower than the entrance ram-recovery ratio of a similar, but smaller, intake located farther forward on a fuselage.

The external drag of the intake approached zero at a mass-flow ratio of approximately 0.7. A similar trend was observed in previous investigations with twin NACA submerged intakes equipped with deflectors and located farther forward.

INTRODUCTION

Information is generally available on the pressure-recovery characteristics of the NACA submerged-type intake located on the forward portion of the fuselage; however, little is known about the pressure-recovery characteristics of this type of intake located toward the rear of the fuselage. Therefore, the pressure-recovery and drag characteristics were obtained for an NACA submerged intake and deflector installation on the rearward portion of the fuselage of a model undergoing tests in the Ames 40- by 80-foot wind tunnel. This report presents the pressure-recovery and drag characteristics of the air-induction system of this model.

SYMBOLS

A	duct area, square feet
d	average duct depth $\left(\frac{A}{w}\right)$, feet
H	total pressure, pounds per square foot
p	static pressure, pounds per square foot
q	dynamic pressure $\left(\frac{1}{2}\rho V^2\right)$, pounds per square foot
S	wing area, square feet
V	velocity of the air stream, feet per second
w	duct width, feet
y	distance from the surface to a point in the boundary layer, inches
α	geometric angle of attack referred to fuselage center line, degrees
δ	boundary-layer thickness where the local velocity is 0.99 of the velocity outside of the boundary layer, inches
ΔC_D	incremental external drag coefficient, based on wing area
ρ	mass density of the air, slugs per cubic foot

Subscripts

o	free stream
1	duct station 1
2	duct station 2
3	duct station 3
4	duct station 4

Parameters

h	the height for which a complete loss of free-stream dynamic pressure would be equal to the integrated loss of total pressure in the actual boundary layer $\left[\int_o^{\delta}\left(\frac{H_o-H}{H_o-p_o}\right)dy\right]$, inches

$\frac{m_1}{m_o}$ the ratio of the mass flow of air in the duct to the mass flow of air in the free stream passing through an area equal to the entrance area of the intake $\left(\frac{\rho_1 A_1 V_1}{\rho_o A_1 V_o}\right)$

$\frac{H-p_o}{H_o-p_o}$ ram-recovery ratio

η duct efficiency $\left(1-\frac{H_1-H_3}{H_1-p_1}\right)$

DESCRIPTION OF MODEL AND APPARATUS

The model with an NACA submerged intake and deflector installation aft of the wing on the bottom of the fuselage is shown mounted in the Ames 40- by 80-foot wind tunnel in figure 1. A schematic drawing showing the general arrangement and the pertinent dimensions of the model is presented in figure 2.

A closeup of the intake and its geometric details are shown in figures 3 and 4, respectively. The ramp plan form was that of the 7° standard curved-diverging ramp described in reference 1. The floor of the 7° ramp was a conical surface. The radius of the cone at the beginning of the ramp (fuselage station 212) was equal to the fuselage radius, and the radius of the cone at the entrance station (duct station 1) was 1.59 of the fuselage radius.

Presented in figure 5 are the shapes and duct areas of the entrance station (duct station 1), the diffuser exit (duct station 2), the plenum chamber (duct station 3), and the outlet (duct station 4). The entrance station was located 6.5 inches downstream from the submerged lip leading edge.

The entrance pressure recoveries and the mass-flow rates were measured by a rake comprised of 40 total-pressure tubes and 5 static-pressure tubes. The entrance rake was removed to determine accurately the pressure recovery in the plenum chamber. This pressure recovery was measured by three static-pressure tubes equally spaced in the vertical plane on the center line of the fuselage. With the entrance rake removed, the mass-flow rates and the pressure losses in the air-induction system were measured at the outlet by a rake consisting of 20 equally spaced total-pressure tubes and 4 static-pressure tubes.

The quantity of air flowing through the air-induction system was varied by changing the size of the orifice at fuselage station 604.

The total-pressure tubes and the static-pressure tubes of each rake were connected to a water-in-glass manometer board, and the pressure

distributions were recorded photographically.

TESTS

The pressure-recovery and incremental-drag characteristics of the NACA submerged intake and deflector installation were determined for a mass-flow-ratio range of approximately 0 to 0.7 and an angle-of-attack range of 0° to 9° at 0° angle of sideslip and at a tunnel airspeed of 125 miles per hour.

The entrance-pressure recovery was measured using the complete model; whereas, due to circumstances not connected with the intake investigation, the external drag of the intake, the internal drag, and the pressure recovery in the plenum chamber were measured with the fuselage alone. For the latter measurements the entrance rake was removed.

RESULTS

Pressure-Recovery Characteristics

The effect of mass-flow ratio on the ram-recovery ratio measured at the entrance and in the plenum chamber is shown in figure 6 for the model at 0° angle of attack. All values of entrance ram-recovery ratio presented in this report were obtained in the manner set forth in reference 2; the total pressure loss indicated by each tube was weighted according to the mass of air flowing through the area apportioned to that tube. It was not possible to measure accurately the entrance ram-recovery ratio below a mass-flow ratio of 0.57 because of the flow angularity, the low inlet velocity, and the small number of tubes. Therefore, at these low mass-flow ratios, the entrance ram-recovery ratio, which is indicated by the dashed line in figure 6, was determined from the plenum-chamber pressure recovery and the duct efficiency. The duct efficiency determined from the total-pressure differential between the entrance and the plenum chamber was found to be the same at mass-flow ratios of 0.56 and 0.67. The duct efficiency was assumed to be constant throughout the mass-flow-ratio range. Figures 7 and 8 show the effect of angle of attack on the ram-recovery ratio at the entrance and in the plenum chamber, respectively.

The distribution of the ram-recovery ratio at the entrance of the NACA submerged intake and deflector installation is presented in figure 9 for two mass-flow ratios at two angles of attack.

Drag of Intake

Figures 10(a) and 10(b) show the effect of mass-flow ratio and angle of attack on the increment of external drag resulting from the addition of the intake to the fuselage. This increment is equal to the external drag of the fuselage with air flowing through the installation minus the drag of the basic fuselage.

The external drag of the fuselage with air flow was taken to be equal to the total drag of the fuselage minus the internal drag determined from pressure measurements. It was assumed that the drag of the fuselage was unaffected by the exiting air. The internal drag coefficient was taken to be equal to

$$2 \frac{A_1}{S} \frac{V_1}{V_o} \left[1 - \sqrt{1 - \left(\frac{H_o - H_4}{q_o} \right)} \right]$$

This equation was derived from a similar equation in reference 3, assuming incompressible flow and basing the drag on wing area instead of fuselage cross-sectional area. The pressure loss term in this equation is a weighted value obtained from the outlet rake readings. It is believed that the accuracy in the measurement of the fuselage drag coefficient is ± 0.0001, and the accuracy of the calculated internal drag coefficient is ± 0.0002.

The drag of the basic fuselage was taken to be equal to the total drag minus the drag resulting from the static pressure differential between the outlet and the ambient air acting on the outlet area. The basic fuselage configuration was the fuselage with the intake sealed and the deflectors protruding and the outlet unfaired. For this configuration it was not possible to remove the deflectors and their effect on the drag is not known. The largest static pressure differential acting on the outlet area existed at 9° angle of attack, and it corresponded to a drag coefficient of 0.0004.

DISCUSSION

Pressure-Recovery Characteristics

Although data are not available to compare the entrance pressure recovery of the intake in this investigation with the pressure recovery of the same intake configuration in a forward location, entrance pressure-recovery characteristics are available for a similar, but smaller, NACA submerged intake located on the forward portion of a fuselage having the same diameter as the one in the present investigation (reference 1). The

leading edge of the intake in the forward location (reference 1) and the leading edge of the intake in the rearward location (fig. 2) were, respectively, 158.25 and 340.50 inches from the beginning of the fuselages. Both these intakes have approximately the same ramp plan forms and the same intake height-to-width ratio, but, as is shown in figure 11, these intakes have different cross-sectional shapes, different duct depths, and different ratios of intake area to fuselage frontal area. The deflectors used on the intake in the present investigation were lower in height than the deflectors used on the intake in the forward location.

In figure 11, the entrance pressure recovery of the intake in the rearward location is compared with the entrance pressure recovery of the intake in the forward location. Because of the difference in the size of deflectors, entrance pressure-recovery data are presented for the forward intake with and without deflectors. If smaller deflectors, comparable in height to the deflectors used on the intake in the present test, had been used on the intake in the forward location, it is reasonable to assume that the resulting entrance pressure recovery of the latter installation would have been between the entrance pressure recovery obtained for that intake with and without deflectors. Based on this assumption, the entrance ram-recovery ratio of the intake in the rearward position is between 0 and 0.05 lower than the entrance ram-recovery ratio of the smaller intake in the forward position.

It is of interest to determine if this difference in entrance ram-recovery ratio can be attributed to the different boundary-layer thicknesses and to the different duct depths. In previous investigations of NACA submerged-type intakes (references 1 and 2), it was determined that a given increase of h/d produced an equal decrease of ram-recovery ratio in the intake. In this parameter, h is the height for which the complete loss of free-stream dynamic pressure is equal to the integrated loss of total pressure in the actual boundary layer, and d is the average depth of the duct at the entrance station. The boundary-layer profile had been measured on the basic fuselage at the entrance station of the intake in the forward location; hence the value of h/d (0.078) was available for this installation. In order to obtain the boundary-layer profile and the corresponding value of h/d for the intake in the rearward location, the turbulent boundary-layer theory for a flat plate was used. The use of this theory for the calculation of the growth and the profile of the boundary layer was justified by the results obtained on a 1/40-scale model of an airship (reference 4). From calculated values of h/d it was determined that, if the smaller intake were moved from the forward to the rearward location, the entrance ram-recovery ratio would be decreased by 0.08 (h/d was increased from 0.078 to 0.155). If the size of the intake were then increased to that of the intake in this investigation, the effect of so reducing the value of h/d alone from 0.155 to 0.079 would be to increase the entrance ram-recovery ratio by 0.08. Thus, the calculations indicate that in this comparison the adverse effect of the thickened boundary layer on the pressure recovery was nullified by the effect of intake depth.

Based on these calculations, it appears that the difference in the entrance ram-recovery ratios of the two intake installations is the result of other factors, such as differences in cross-sectional shape and differences in the ratio of intake area to fuselage frontal area.

The effect of angle of attack on the entrance pressure recovery of the intake in the rearward location is small (fig. 7); at a mass-flow ratio of 0.74, increasing the angle of attack from 0° to 9° increased the entrance ram-recovery ratio by 0.03. This change in ram-recovery ratio due to intake attitude is equal to the change in entrance ram-recovery ratio resulting from a comparable change in the sideslip attitude of a single side intake in the forward location (reference 5).

Drag of the Intake

From the data presented in this report, it is not possible to determine the effect of intake location on the external drag of the intake because of the differences in intake geometry and in the method of obtaining the drag of previous installations. The incremental external drag coefficients presented in this report should be used qualitatively because they were determined from measurements made with the deflectors on the sealed fuselage. However, the approach of the drag increment to zero at a mass-flow ratio of approximately 0.7 (see fig. 10(a)) is in agreement with available data for a twin NACA submerged intake and deflector installation in a forward location (reference 6). The results presented in reference 1 indicate the detrimental effect, on the performance of an airplane, of adding deflectors to an NACA submerged intake installation.

CONCLUDING REMARKS

The results of this investigation indicated that the entrance ram-recovery ratio of the NACA submerged intake and deflector installation on the rearward portion of the fuselage was between 0 and 0.05 lower than the entrance ram-recovery ratio of a similar, but smaller, intake located farther forward on a fuselage. Calculations indicate that the effect of the thicker boundary layer on the pressure recovery of the intake in the rearward location was nullified by the effect of the greater depth of that intake.

The variation of the entrance ram-recovery ratio with angle of attack was small, and it was equivalent to the variation that had been obtained with an NACA submerged intake in a forward location.

The external drag of the intake with deflectors in this investigation was similar to that of a twin-intake installation in a forward

location in that the external drag of the intake approached zero at the higher mass-flow ratios.

Ames Aeronautical Laboratory,
National Advisory Committee for Aeronautics,
Moffett Field, Calif.

REFERENCES

1. Martin, Norman J., and Holzhauser, Curt A.: An Experimental Investigation at Large Scale of Several Configurations of an NACA Submerged Air Intake. NACA RM A8F21, 1948.

2. Mossman, Emmet A., and Randall, Lauros M.: An Experimental Investigation of the Design Variables for NACA Submerged Duct Entrances. NACA RM A7I30, 1948.

3. Becker, John V.: Wind-Tunnel Tests of Air Inlet and Outlet Openings on a Streamline Body. NACA ACR, Nov. 1940.

4. Freeman, Hugh B.: Measurements of Flow in the Boundary Layer of a 1/40-Scale Model of the U.S. Airship "Akron." NACA Rep. 430, 1932.

5. Martin, Norman J., and Holzhauser, Curt A.: An Experimental Investigation at Large Scale of Single and Twin NACA Submerged Side Intakes at Several Angles of Sideslip. NACA RM A9F20, 1949.

6. Hall, Charles F., and Barclay, F. Dorn: An Experimental Investigation of NACA Submerged Inlets at High Subsonic Speeds. I - Inlets Forward of the Wing Leading Edge. NACA RM A8B16, 1948.

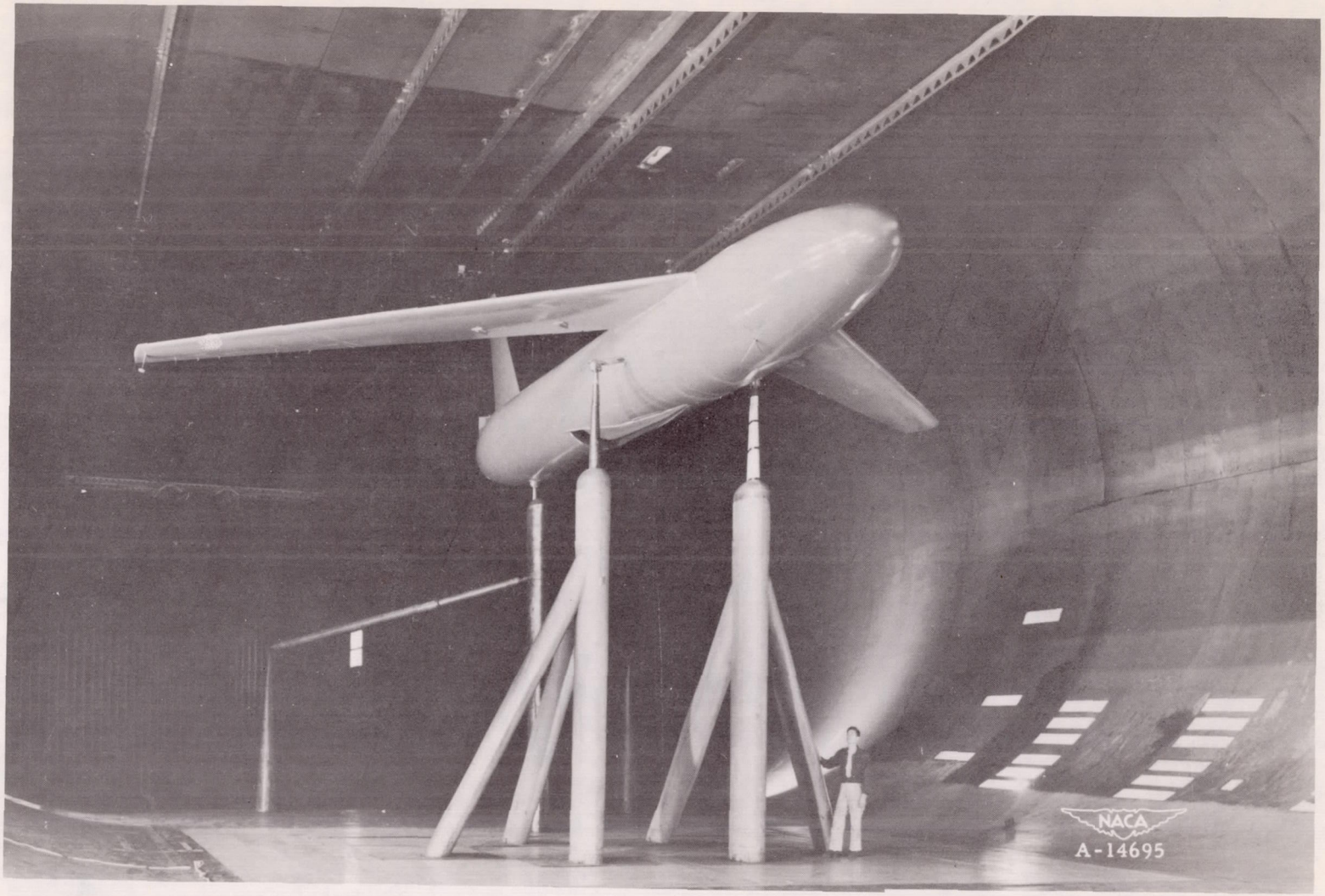

Figure 1.– The model with an NACA submerged intake and deflector installation.

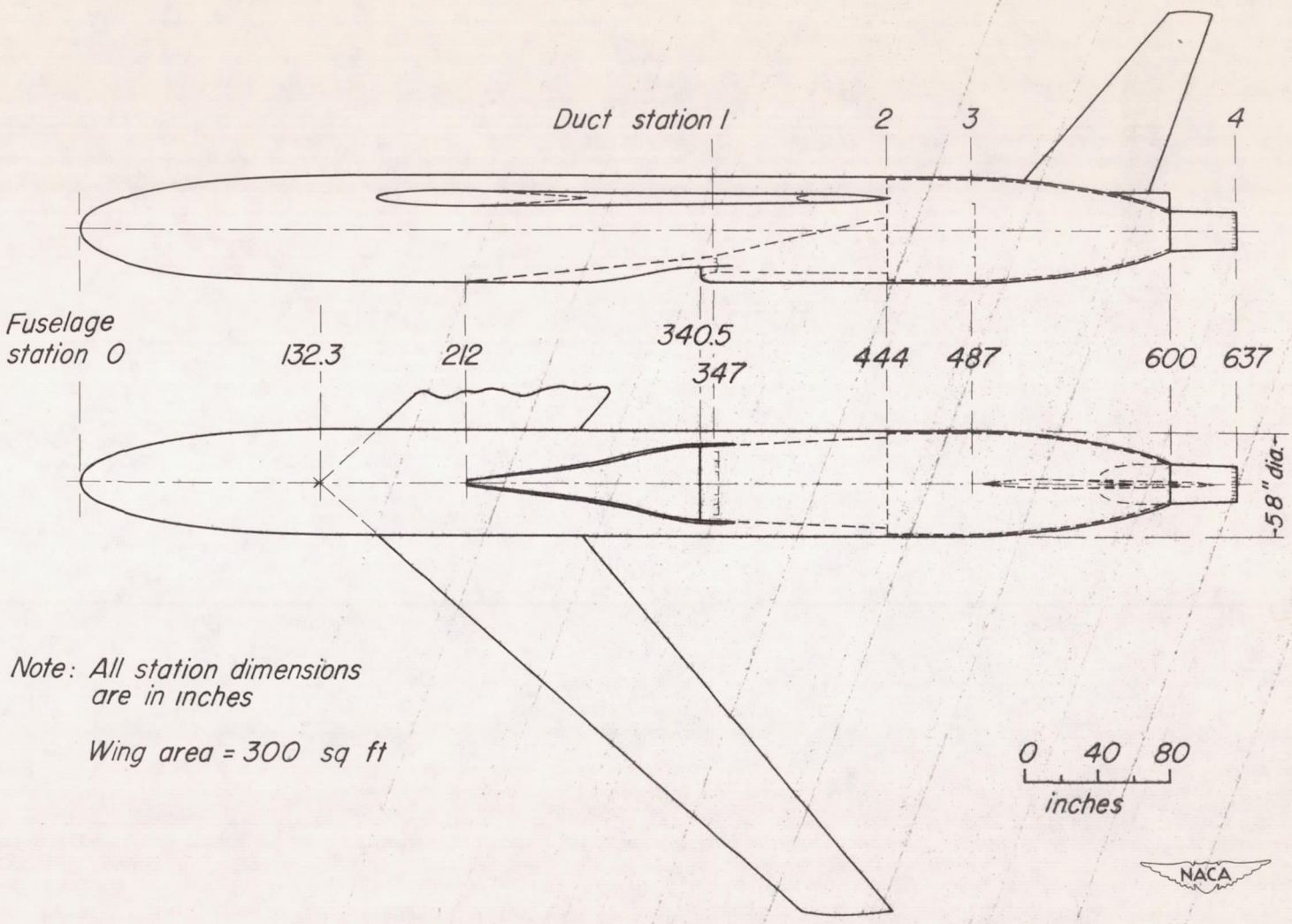

Figure 2.- Schematic drawing showing arrangement of the model with an NACA submerged intake and deflector installation.

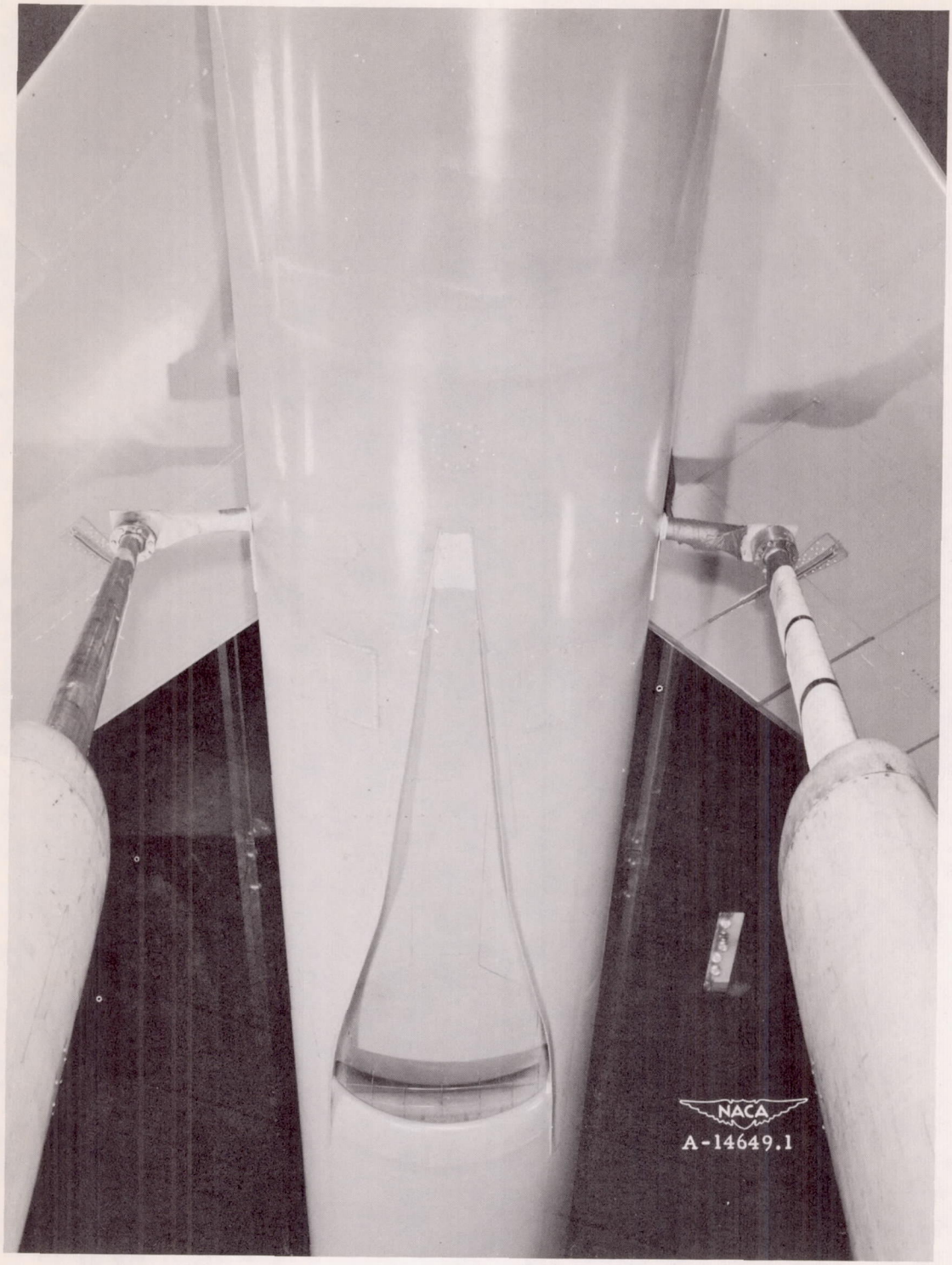

Figure 3.– Close–up of the intake.

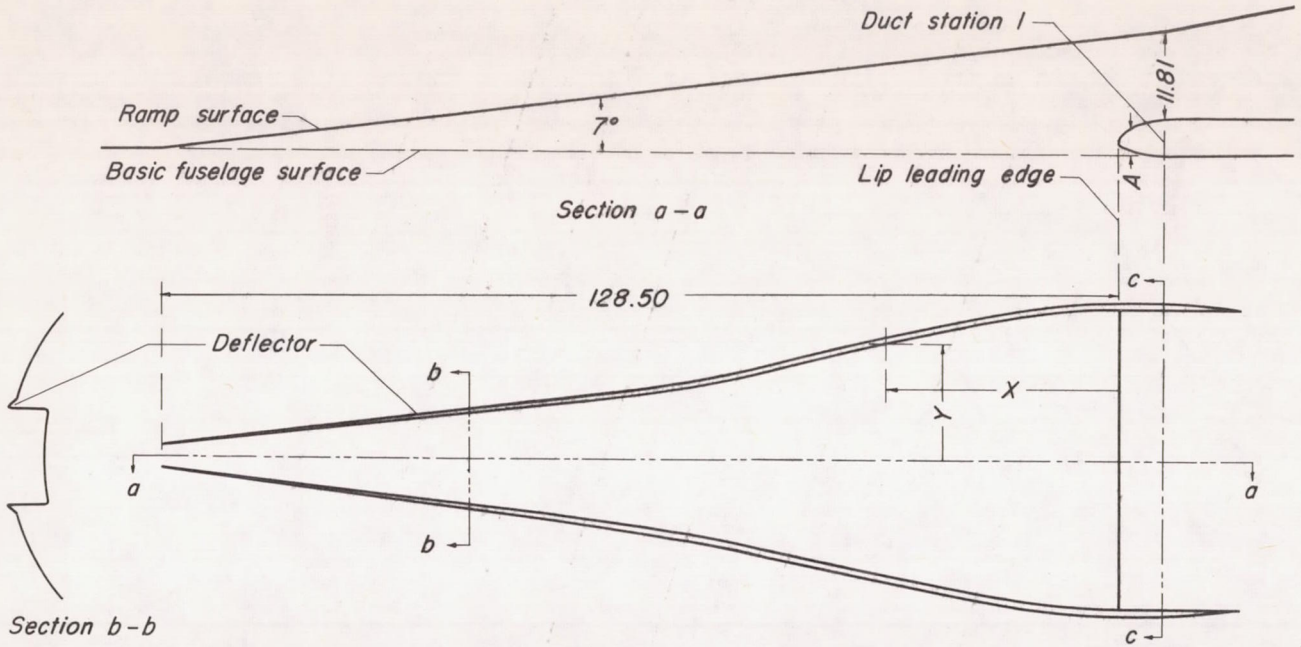

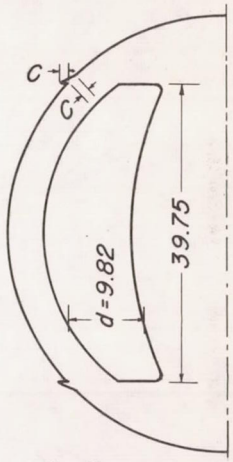

Ramp coordinates	
X	Y
128.50	1.702
107.30	2.860
74.00	4.085
60.00	9.450
46.30	12.250
32.60	15.205
18.90	17.970
13.50	18.712
0	19.875

Lip coordinates		
X	A	B
0.00	2.060	2.060
-1.30	3.370	.903
-2.60	3.900	.575
-3.90	4.285	.350
-5.20	4.563	.213
-6.50	4.752	.120
-7.80	4.840	.060
-9.10	4.840	.015
-10.40	4.833	0

Deflector coordinates		
X	C	D
128.50	0.00	0.00
107.30	.40	.06
74.00	.79	.10
60.00	1.00	.13
↓	1.00	.13
-8.50	1.00	.13
-12.96	.73	.08
-18.00	0	0

All dimensions are in inches

B is distance from basic fuselage surface to external surface of the lip

D is the radius on the corner of the deflector

NACA

Figure 4. - Details of the ramp, lip, and deflectors tested on the model.

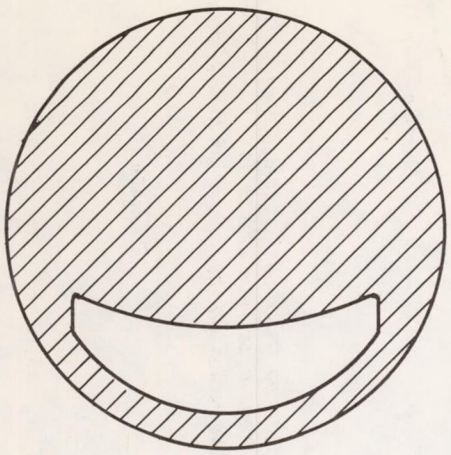

Duct station 1
Duct area = 2.71 sq ft

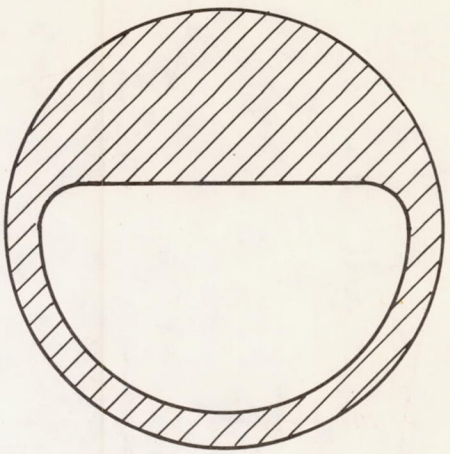

Duct station 2
Duct area = 8.96 sq ft

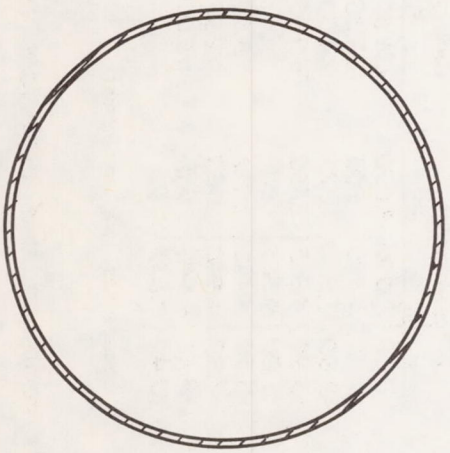

Duct station 3
Duct area = 17.12 sq ft

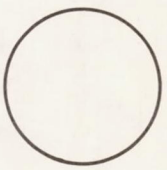

Duct station 4
Duct area = 2.14 sq ft

Figure 5. - Fuselage cross sections at duct stations 1, 2, 3, and 4.

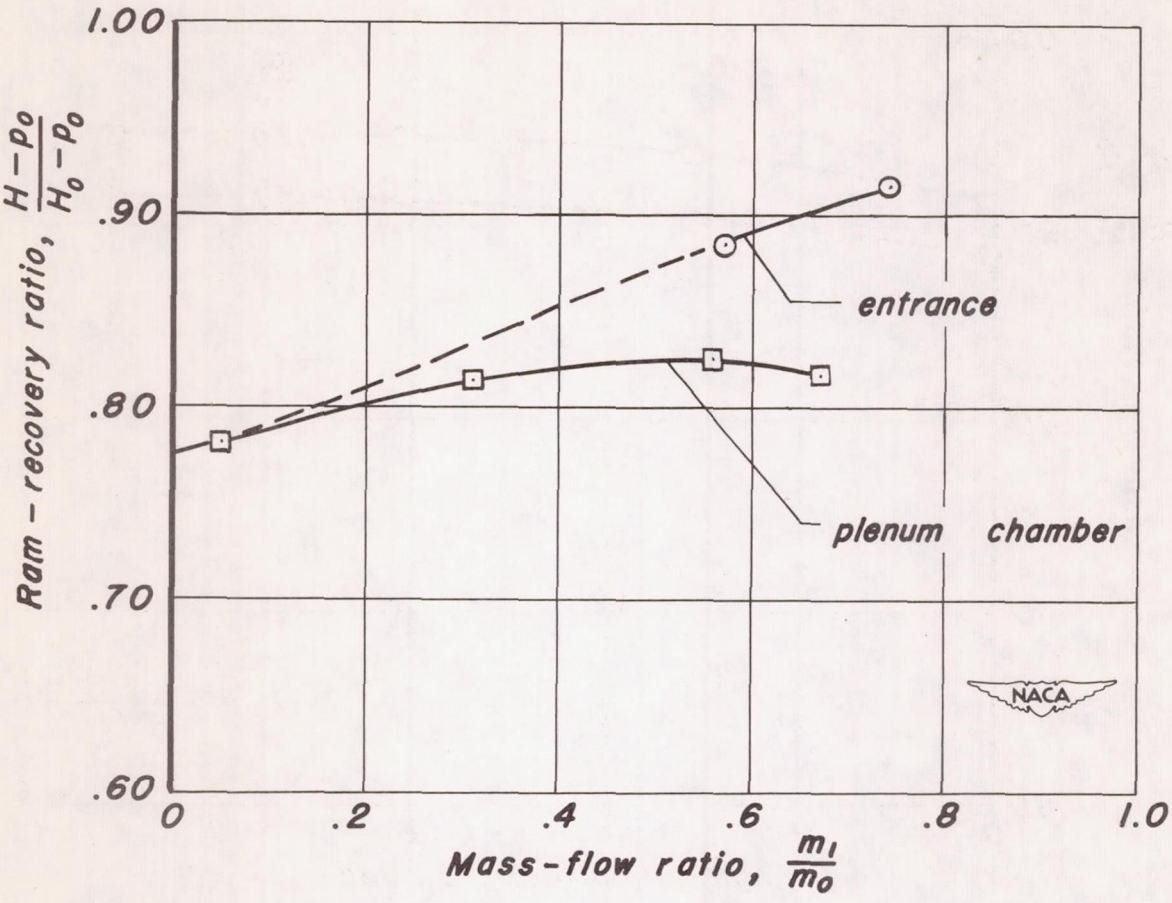

Figure 6. -The effect of mass-flow ratio on the ram-recovery ratio measured at the entrance and in the plenum chamber, $\alpha = 0°$.

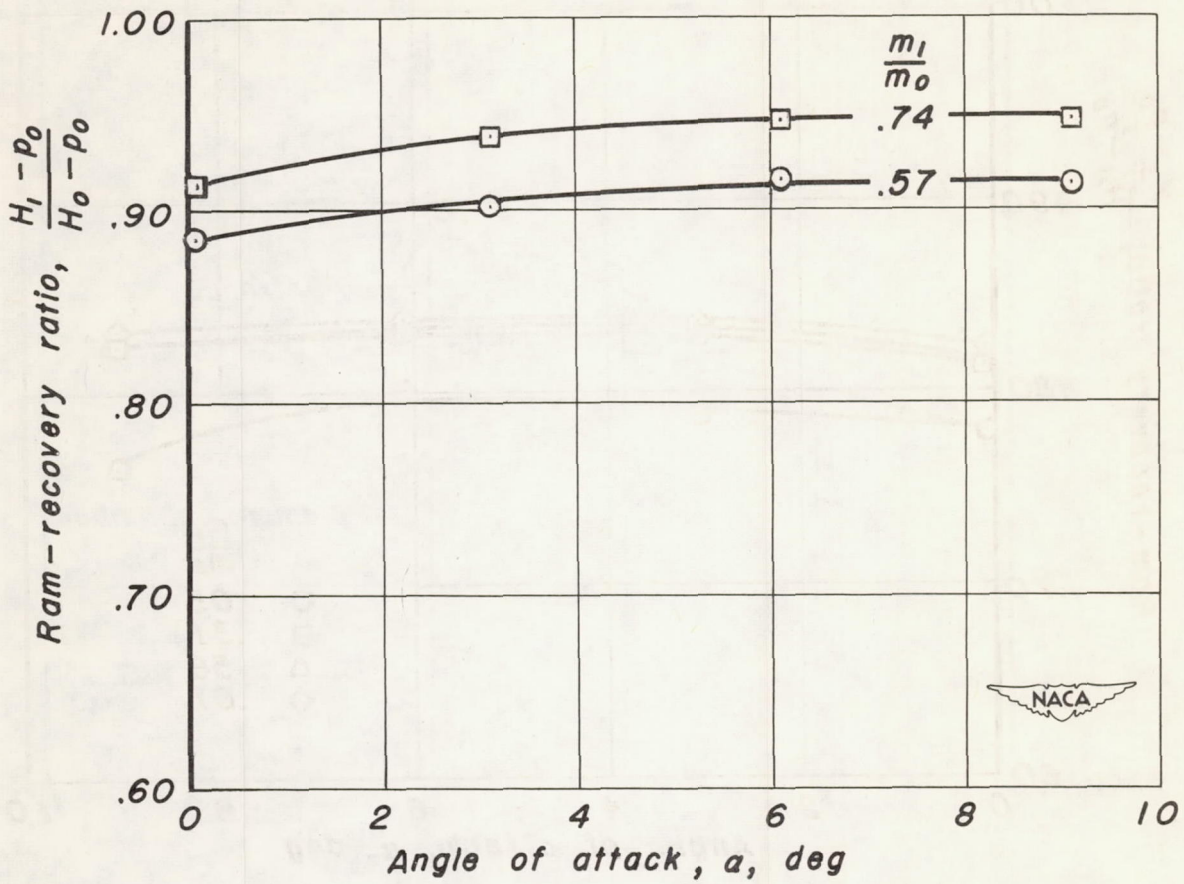

Figure 7. -The variation of entrance ram-recovery ratio with angle of attack.

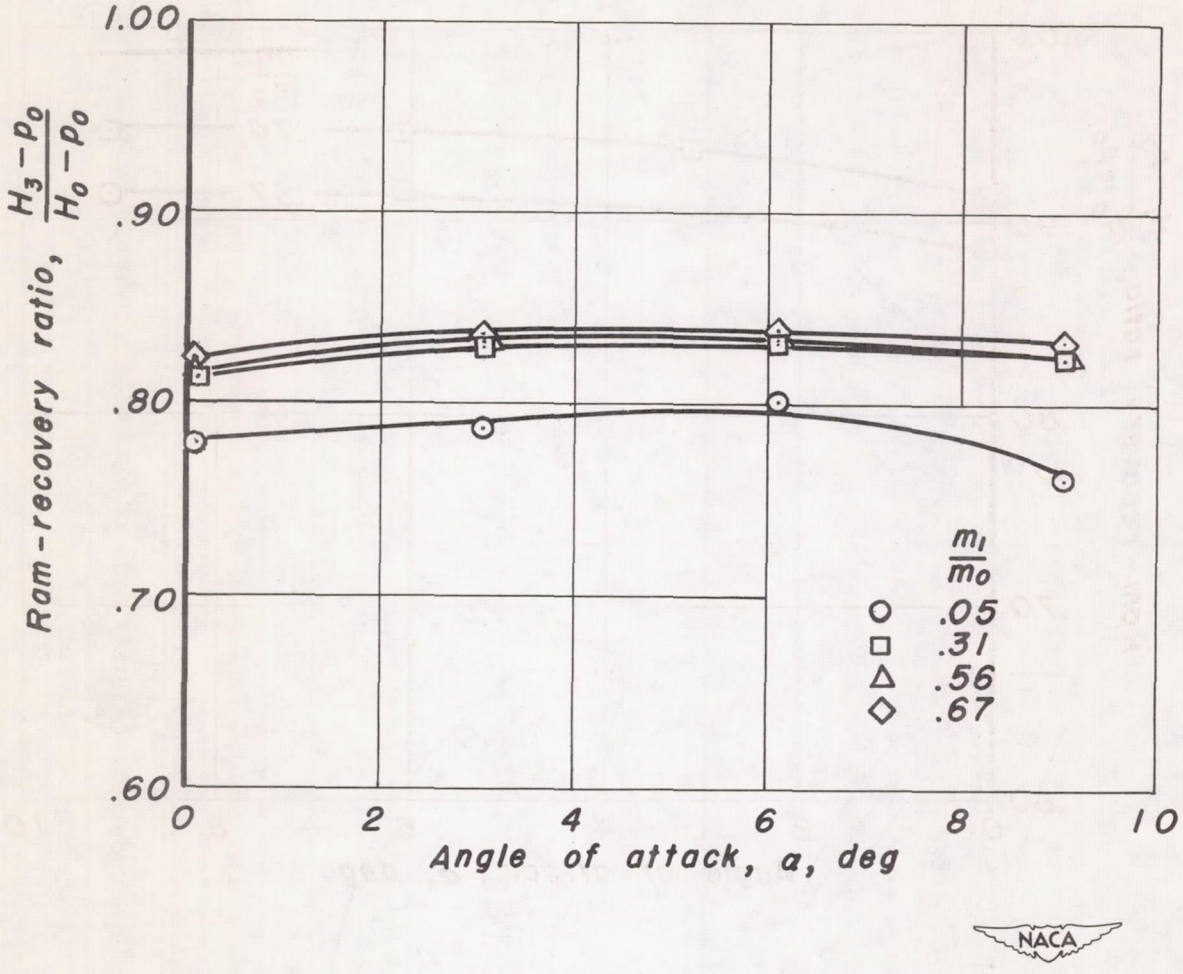

Figure 8. -The effect of angle of attack on the ram-recovery ratio in the plenum chamber.

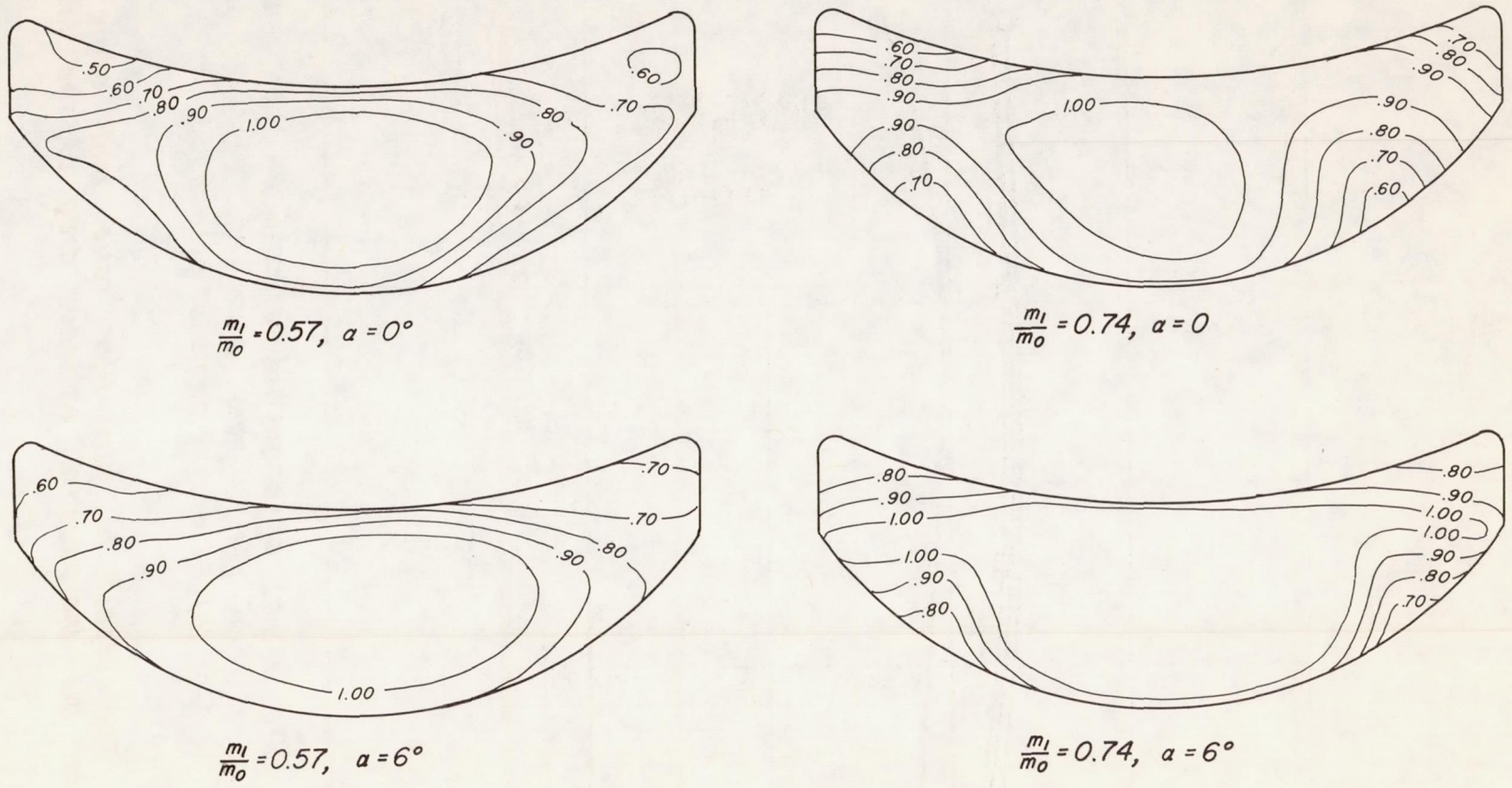

Figure 9. – Distribution of entrance ram-recovery ratio of the NACA submerged intake with deflectors.

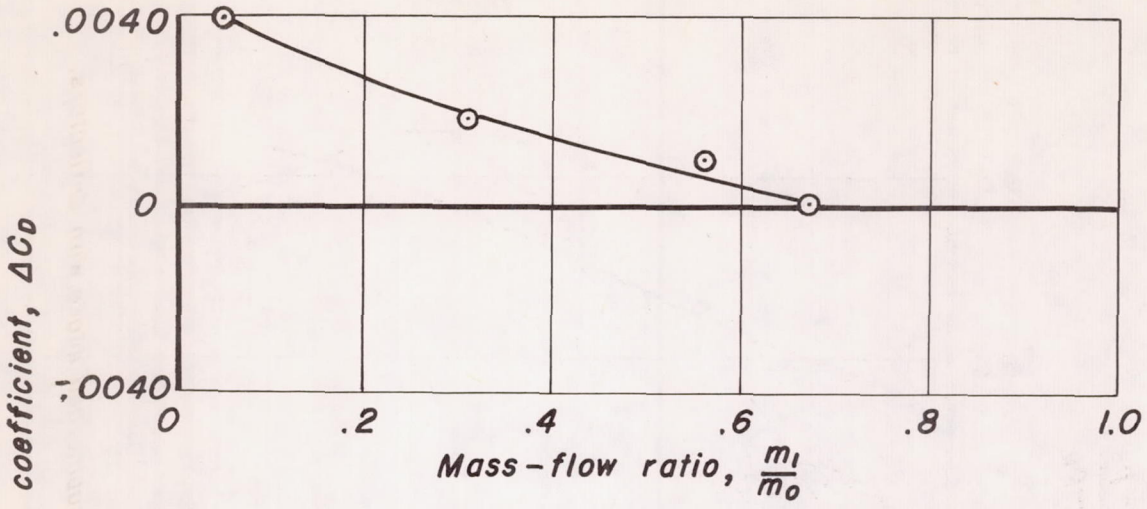

(a) Effect of mass-flow ratio, $\alpha = 0°$.

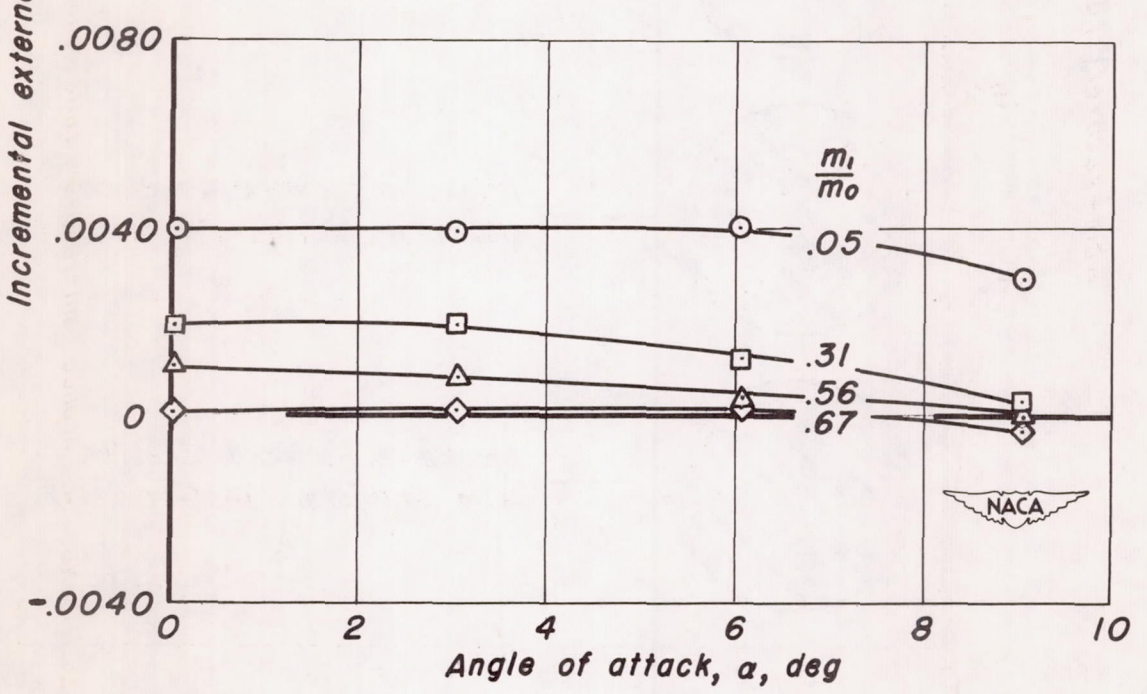

(b) Effect of angle of attack.

Figure 10. -The effect of mass-flow ratio and angle of attack on the incremental external drag of the intake.

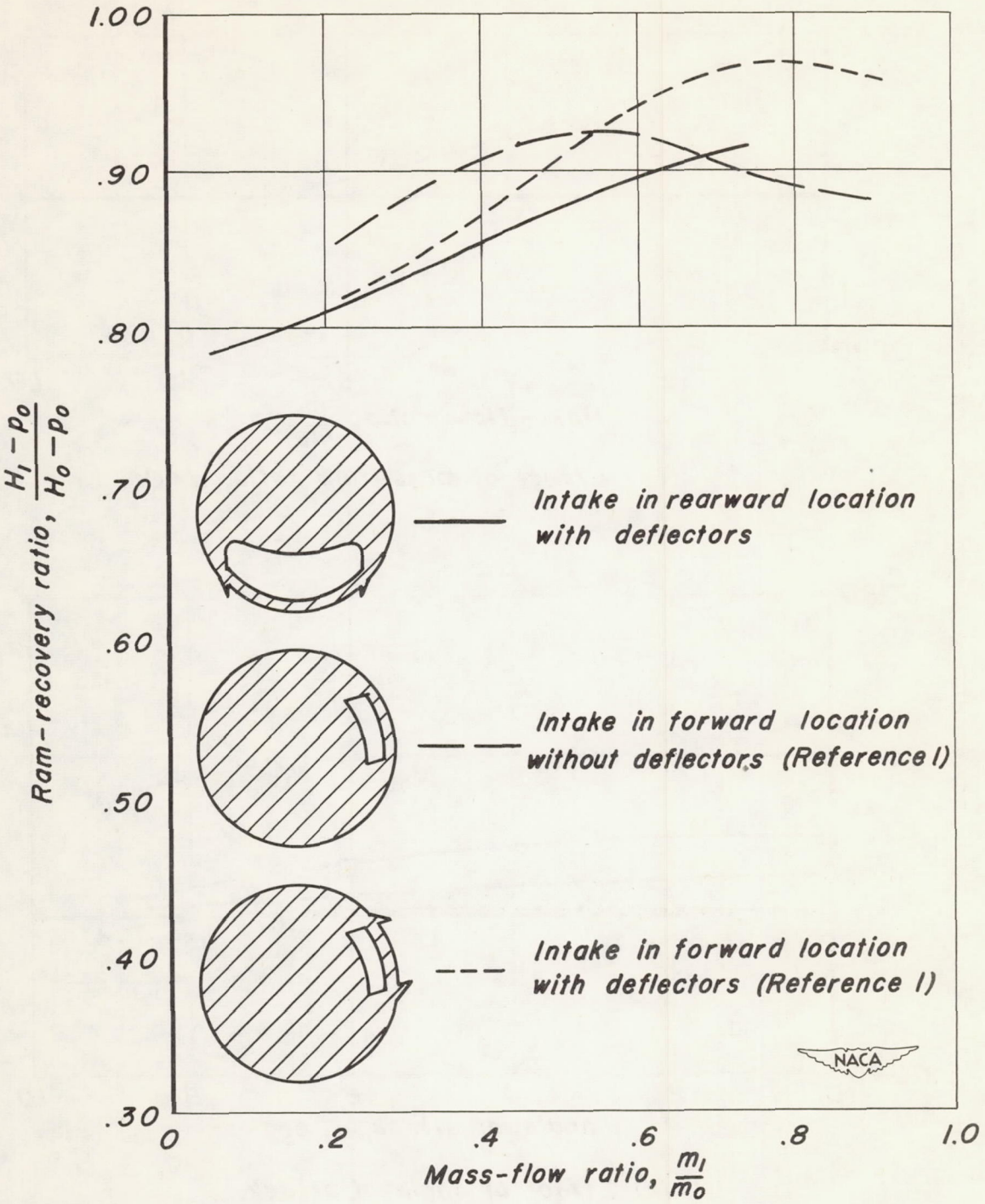

Figure 11. -Comparison of the entrance ram-recovery ratios of two NACA submerged intake installations, $\alpha = 0°$.